Domestic biogas digesters reduce greenhouse gas emissions and provide benefits to households

The Clean Development Mechanism (CDM) is an important instrument for reducing greenhouse gas (GHG) emissions because it provides for carbon offset projects in developing countries. However, this system is not working well due to the low price of carbon credits and so on. Thus, for the mitigation technology to be disseminated widely, it should be beneficial to households. The installation of domestic biogas digesters (BDs) using mainly livestock manure (Fig. 1) is one of the mitigation actions that can be applied at the household scale. This research, therefore, aims to clarify 1) whether BD is a measurable, reportable, and verifiable mitigation technology, and 2) whether BD realizes both mitigation and household benefits.

BDs were installed in 435 households in Mekong Delta, Vietnam, and the annual monitoring results (from 1 June 2013 to 31 May 2014) of biogas usage revealed that they used biogas for cooking on 95.7% of the total number of days. During this period, a total of 446 tCO_2 of GHG were reduced by substituting conventional cooking fuel with biogas. This amount of reduction was verified and approved by the UNFCCC CDM Executive Board, and carbon credits were issued on 19 June 2015. This confirms that GHG emission is reduced by introducing BDs, and that it is a measurable, reportable, and verifiable climate change mitigation technology.

Introducing BDs reduced the amount of firewood and LP gas used (Fig. 2). GHG emission reduction and cooking fuel savings per household were estimated at 1.87 tCO_2 and USD95, respectively, based on the annual changes in the usage amount of conventional cooking fuel (Table 1). Moreover, households that adopted BD technology benefitted financially. Questionnaire results indicated that more than 99% of households were satisfied with the introduction of BDs. Participating households also evaluated the effects of BD introduction, which included cost savings on cooking fuel, time savings due to less time spent on firewood collection, health benefits from avoiding smoke or soot generated by cooking with firewood, and environmental enhancements such as avoiding malodors and overcoming poor water quality issues (Fig. 3). The abovementioned results confirm that in addition to being a measurable, reportable, and verifiable mitigation technology for climate change, BD use also reduces greenhouse gas emissions and provides benefits to households.

The results of this research will form the basis of the suggestions that will be provided to the Vietnamese government when they try to realize their Intended Nationally Determined Contributions (INDC), which mentioned the use of biogas as among its GHG emission reduction strategies from the agricultural sector. Quantifying GHG emission reduction and household benefits derived by the installation of BDs depends on the amounts and types of cooking fuel used by the households prior to BD installation. The BD’s total initial cost is estimated at around USD180 (BD unit = USD140; labor = USD20; technical support = USD20), while maintenance cost is estimated at around USD20 per year. Considering the discount rate, the BD’s net present value during its useful life (about 7 years) can thus be

calculated as more than USD200, which is nearly equal to two years' worth of cooking fuel expenses for one household.

(T. Izumi)

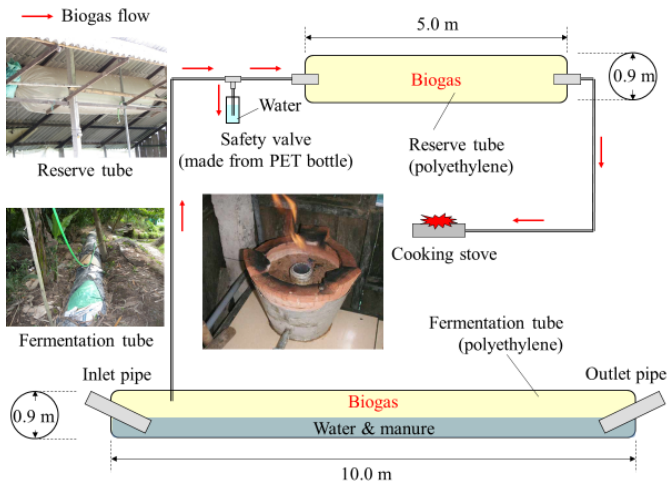

Fig. 1. Plastic biogas digester (BD) system

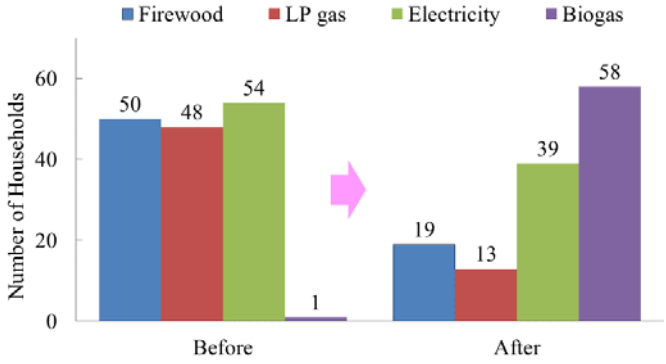

Fig. 2. Changes in cooking fuel usage before and after biogas digester (BD) installation

Note 1. Total number of surveyed households: 66
Note 2. Y-axis values refer to number of households that used each cooking fuel type during the study period
Note 3. One household used biogas digester (self-installed before project initiation)

Table 1. Changes related to farm household cooking fuels before and after biogas digester (BD) installation

(One household, Average of 66 households)

Item			Before	After	Difference
Amount of cooking fuel used	Firewood (t year^{-1})	Cooking	1.59	0.32	-1.27
		Pig feed	1.50	0.38	-1.12
		Total	3.09	0.70	-2.39
	LP gas (kg year^{-1})		27.3	2.4	-24.9
GHG emissions (tCO_2 year^{-1})	Firewood	Cooking	1.20	0.24	-0.96
		Pig feed	1.13	0.29	-0.84
		Total	2.33	0.53	-1.80
	LP gas		0.08	0.01	-0.07
	Total		2.41	0.54	-1.87
Expenses for cooking fuel (USD year^{-1})	Firewood (purchase)		14	1	-13
	Firewood (collection)		53	12	-41
	LP gas		45	4	-41
	Total		112	17	-95

Note. Survey on cooking fuel expenses was conducted based on Vietnamese currency (VND) and converted to US dollar using the exchange rate as of survey period (from 2012 to 2014).

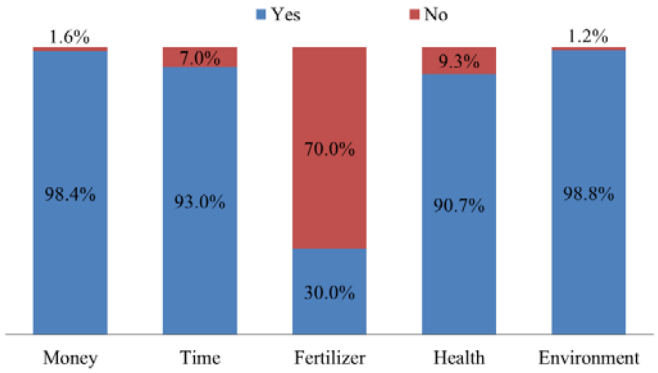

Fig. 3. Perceptions of participating households regarding the effects of biogas digester (BD) installation

Note 1. Number of surveyed households: 257
Note 2. Money = cost savings on cooking fuel; Time = time savings associated with reduced time spent on firewood collection and cooking; Fertilizer = use of BD effluent as fertilizer for gardens and ponds; Health = health benefits from avoiding smoke and soot generated from cooking by firewood; Environment = Environmental enhancement by reducing malodors and overcoming poor water quality issues.

A-02

Estimation of cost and effect of food policy to mitigate rice price variation under climate change in Bangladesh

Bangladesh is located downstream of large international rivers and along the path of tropical storms, making the country prone to natural disasters and its agricultural production unstable. According to recent meteorological observations, the frequency of higher temperatures is increasing, and climate change is projected to affect the crop yields more severely in the future. To cope with the instability in agricultural production, policy tools for climate change adaptation as well as adaptation technology development are important. In this study, we estimated the cost and effect of procurement and distribution policies in mitigating rice price variation under climate change.

To estimate the policy cost and effect, we developed a rice supply-demand model in Bangladesh, based on analysis of statistical data related to paddy area, rice production, price, import and export, stock level, GDP, and population. We also estimated the yield functions of different seasonal rice, based on yield statistics and meteorological data, so we can forecast climate change impacts on rice yield. To analyze the policy, we added a policy model consisting of procurement and distribution functions. By assuming that the amount of procurement and distribution are decided by farmers' and consumers' decision-making on trade partners, with the difference between governmental and market prices as the main incentive and subject to physical constraints related to rice storage capacity and actual stock, we can apply the Tobit model to estimate procurement and distribution functions.

We made outlooks under the IPCC climate RCP6.0 and socioeconomic SSP2 scenarios, with 2010 to 2030 as the forecast period. When inputting future climate data from the global circulation model (MIROC5) into the yield model, rice yields show an increasing trend in the ranges of variation (Table 1 and Fig. 1), implying greater rice market instability and food policy importance. Figure 2 shows two rice price forecasts. The green line shows baseline and the blue line shows a new policy in which more intensive policy intervention is conducted by reducing the distribution price and increasing the procurement price when the price difference from the trend line is more than 10%. As the figure shows, the new policy reduces the range of price variation. Reduction in price variation is almost 2.34% points (Table 2). Additional policy costs per year for this variation reduction are estimated to be US$14 million for facility construction and maintenance, US$195 million for rice stock quality maintenance, and US$183 million for rice transaction. In addition, storage capacity needs to be increased from 1.7 million tons to 3 million tons.

There are some other climate change and socioeconomic scenarios and different global circulation models. Therefore, the result of this study based on certain scenarios and a model is not the sole outlook. However, this result can provide basic information for food policy making in the era of climate change and for assessing adaptation technologies.

(S. Kobayashi, J. Furuya, Md. A. Salam [University of Tsukuba], Md. S. Alamgir [UT])

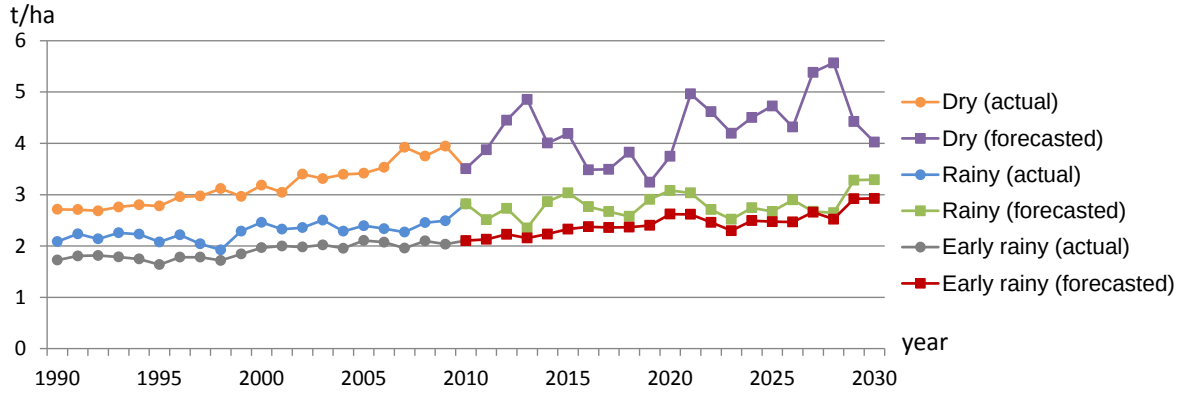

Fig. 1. Actual and forecasted rice yields of improved varieties for different rice seasons

Table 1. Rice yield variation and climate change impact

Rice season	Coefficient of variation (%)		Climate impact
	Until 2009	2010 - 2030	(% point)
Early rainy (Aus)	8.32	9.30	0.98
Rainy (Aman)	7.76	8.72	0.96
Dry (Boro)	12.28	14.6	2.32

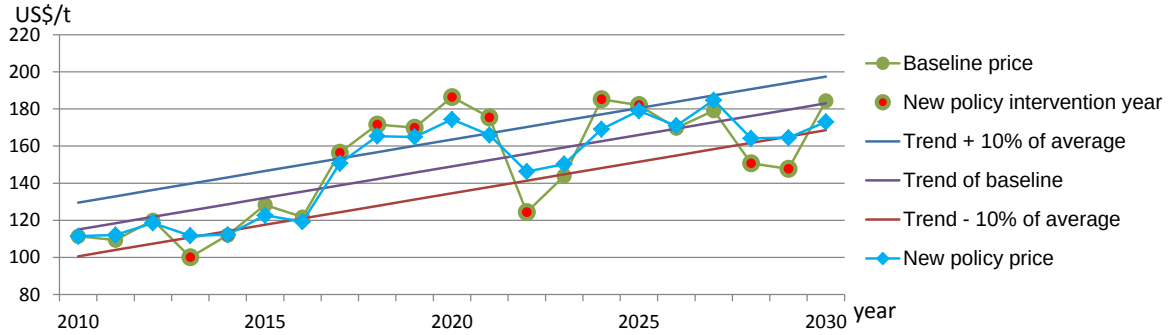

Fig. 2. Stabilization of rice price by an intensified food policy (farm gate price)

Table 2. Rice price variation and policy effect

Price type	Coefficient of variation (%)		Policy effect
	Baseline	New policy	(% point)
Farm gate	19.85	17.50	–2.35
Retail	25.75	23.42	–2.33

A-03

Calcination improves solubility of low-grade African phosphate rock and application of calcined products is highly effective on crop cultivation

The utilization of local African phosphate rock (PR) can be considered a key factor in solving hunger and poverty in Africa through improvement of crop productivity. It is well known that large amounts of phosphate deposits exist in Sub-Saharan Africa, with reserve estimates of around 100 million tons of P_2O_5 in Burkina Faso. However, this PR resource has not been fully utilized because of limited solubility. Numerous studies have attempted to utilize these low-grade PRs with various crops, and results have indicated that the direct application of PR exhibits substantial variation in effectiveness, reflecting the influence of various factors such as PR solubility, soil properties, and the types of crops.

For the abovementioned reason, an effective solubilization method for these PR is highly required. Sulfuric acid addition is the most popular solubilization method, and sulfuric acid is also used for partial acidulation of PR. However, in the case of low-grade African PR, the partial acidulation method is potentially problematic because of the low solubilization rate and the accumulation of residual free sulfuric acid.

We attempted to solubilize low-grade PR produced in Burkina Faso using Akiyama's calcination method, which was previously developed for high silicate PRs. Results showed that PR calcination between 900-1000 °C with composition of 25-30% Na_2O sourced by sodium carbonate (Na_2CO_3) solubilized PR effectively. Phosphorus (P) solubility in 2% citric acid solution was leached about 100%, and P solubility in water was increased to 28%.

Results also clarified that higher composition of Na_2O increases solubility in 2% citric acid and in water. On the other hand, adding larger amounts of sodium carbonate consequently decreases total P_2O_5 content in calcined PR.

Furthermore, the effects of calcined Burkina Faso PR (CBPR) application on rice and maize growth were evaluated through a pot experiment. CBPR calcined at 950 °C with 30% Na_2O was investigated for this pot experiment. Lowland rice and maize were cultivated for 56 days under four levels of P_2O_5 application, i.e., 0.0, 0.5, 1.0, and 2.0 g P_2O_5 /pot. Nitrogen and potassium were applied using 1g N and 1 g K_2O per pot. CBPR application for lowland rice indicated comparable effect with Triple Super Phosphate (TSP) application at application rates of up to 2 g P_2O_5/pot. In the case of maize, CBPR application yielded about 40% of TSP application.

Crop productivity improvement in Africa would be highly expected through provision of affordable fertilizer using low-grade African PR. Calcination technology is likely to be applicable not only for Burkina Faso PR but also for all other low-grade PRs in Africa.

(S. Nakamura, F. Nagumo, M. Fukuda, K. Toriyama, T. Imai [Taiheiyo Cement Corporation])

Table 1. Total P_2O_5 content and solubility for citric acid and water of calcined PR

Treatment	Temp. of calcination	Total P_2O_5 content in calcined PR	Rate of citric acid soluble P against total P in calcined PR	Rate of water soluble P against total P in calcined PR
	°C	g kg^{-1}	%	
Burkina PR (Untreated)		297.1	31.1	0.2
Na20	950	227.2	73.3 a	0.5 a
	1000	231.5	73.9 a	0.5 a
Na25	850	205.8	81.8 a	17.1 b
	900	207.5	93.5 ab	17.2 b
	950	211.8	99.8 b	16.0 b
	1000	212.7	100.0 b	8.3 a
Na30	850	189.5	92.6 a	27.1 a
	900	186.9	96.8 ab	28.0 a
	950*	197.2	97.5 b	28.1 a
	1000	198.1	98.7 b	26.7 a

Na20, Na25, Na30 indicate Na_2O treatment compositions at 20%, 25%, and 30%, respectively. Different alphabets denote significant difference ($p < 0.05$) among calcination temperatures using Tukey's multiple comparison (n=3). *Calcined PR of Na30 at 950 °C was used for the subsequent pot experiment.

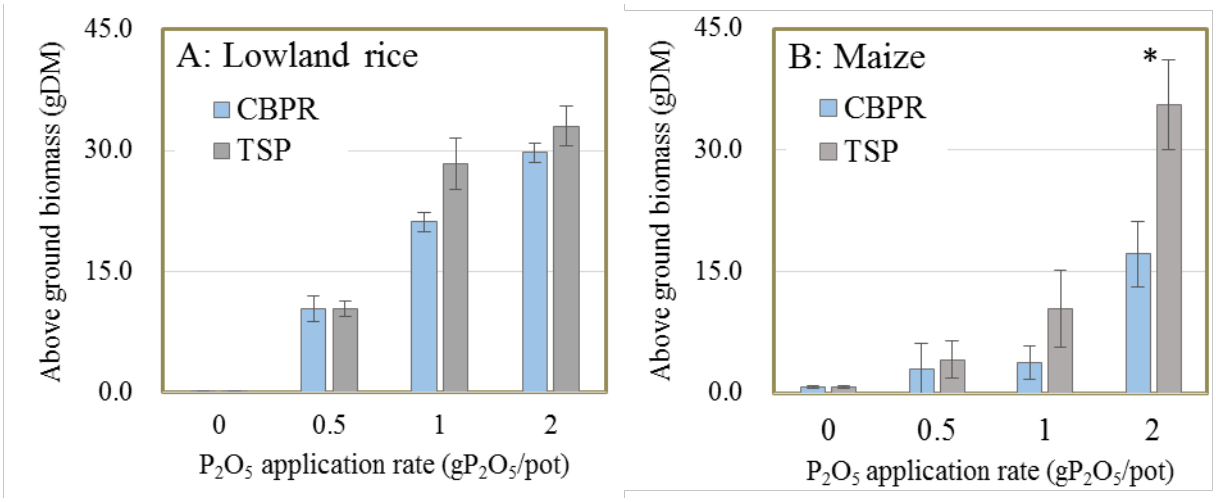

Fig. 1. Effect of applying calcined PR and TSP on aboveground biomass yield of lowland rice (A) and maize (B)

CBPR: Calcined Burkina Faso phosphate rock, TSP: Triple super phosphate. Error bars are standard errors (n=3). Asterisk in the figure denotes significant difference ($p < 0.05$) between yields of CBPR and TSP using Student's t test.

B-01

Application of infrared spectroscopy for rapid prediction of crude protein content in cowpea (*Vigna unguiculata*) grain

Cowpea is a staple grain legume widely cultivated in Africa, playing key roles in the region as a food crop for the people and as an important cash income source for farmers. In addition to ongoing efforts toward improving crop productivity and insect-pest resistance, focus is also being placed on enhancing the grain quality and nutritional value of crops with multiple roles, especially cowpea, which serves as the primary source of protein in the region. Protein content is one of the most important grain quality traits, and significant protein content in grains can have a major impact on the livelihoods of people in the region. In this work, we focused on the crude protein content of grain as a primary nutritional property, and we developed a suitable prediction method that can be used in the breeding process and in evaluating environmental effects.

A total of 919 ground grain samples from 224 lines covering the genetic diversity in grain nitrogen content of the crop were used for the development of a calibration model to predict nitrogen content (Fig. 1). The developed infrared spectroscopy model using the actual nitrogen content obtained by the Dumas combustion method and the near-infrared (4000-4985cm^{-1}) and mid-infrared (1400-2290 cm^{-1}) spectroscopy obtained by Fourier Transform Infrared Spectrometer had reasonable accuracy (R^2 = 0.91). The model also predicted the nitrogen contents of the grain samples grown in three agro-ecological zones across major cowpea-growing areas in West Africa with acceptable accuracy (R^2 = 0.90-0.92) (Fig. 2 and Table 1). Obtained nitrogen contents can be accurately converted to crude protein content using a nitrogen-to-protein conversion factor of 5.45 developed for cowpea based on the relationship between amino acid composition and nitrogen content using 20 selected cowpea lines (Fig. 3). The developed method using infrared spectroscopy can predict crude protein content in cowpea grain in a time-effective manner (approx. 100 sec./sample) compared to the standard Dumas convection method (approx. 870 sec./ sample) including the time for sample loading.

The method’s cost- and time-effectiveness should enable cowpea breeders in West Africa to select potential parental materials and conduct effective breeding with a focus on grain protein content. Also, the method provides useful tools for field agronomic studies, which in turn should help us understand the environmental effects on grain protein content and allow further development of suitable cultivation techniques to produce quality cowpea grains in each region.

(S. Muranaka, M. Shono, H. Ishikawa [International Institute of Tropical Agriculture])

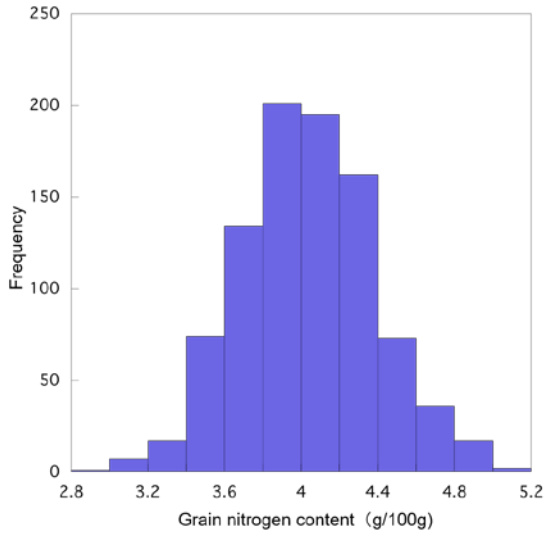

Fig. 1. Distribution of grain nitrogen content of the 224 lines used for the development of the model

Table 1. Variation statistics of the developed model for predicting grain nitrogen content

Validation set	R^2	RMSEP	RPD
All samples	0.93	0.10	3.68
Each agro-ecological zone			
Ibadan (Savanna-forest transition)	0.90	0.09	3.13
Minjibir (Sudan savanna)	0.92	0.09	3.40
Toumnia (Sahel)	0.92	0.10	3.46

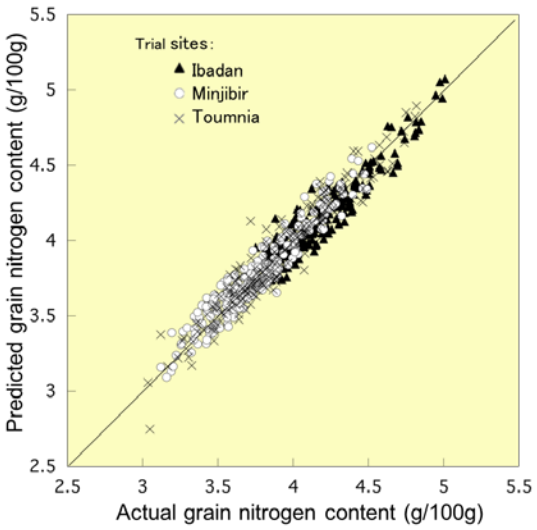

Fig. 2. Validation of the developed model for determining the nitrogen content of grain samples collected from different agro-ecological zones in Ibadan, Minjibir and Toumnia

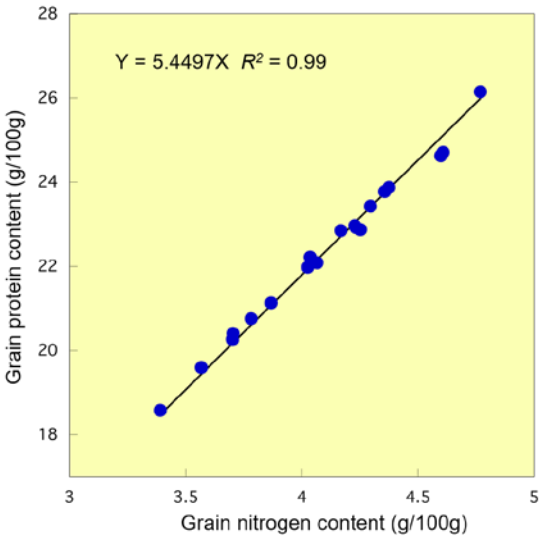

Fig. 3. Relationship between actual protein content and nitrogen content of 20 selected cowpea lines

An optimal heat inducible synthetic promoter in plants

Climate change is predicted to adversely affect agriculture. There is a growing need for the development of crops capable of adapting to change. At the molecular level, one of the most discussed environmental conditions is high temperature or heat shock (HS). Many genes have been described that respond to HS stress at the transcriptional level, and their gene products are thought to function in stress tolerance. Heat shock factors (HSFs) bind heat shock response elements (HSEs) with the core sequence to form trimers, thereby regulating downstream gene expression. The importance of the HSF–HSE interaction has previously been suggested in the HS response. However, because plant HSFs are involved not only in HS but also in water deficit stress, development, cell differentiation, and proliferation, it has been suggested that the induction of HS requires a specific combination of HSFs and HSEs.

In this study, to determine representative HS-responsive transcriptional pathways in plants, we analyzed HS-responsible genes and promoters in *Arabidopsis*, soybean, rice, and maize. We also designed an optimized HS-inducible promoter based on detailed bioinformatics predictions of conserved sequences (*cis*-acting elements) from HS-inducible promoters of these four plant species for molecular breeding purposes.

First, to characterize plant HS-responsive genes, a transcriptome analysis of *Arabidopsis*, soybean, rice, and maize was conducted using microarrays. Second, we used our in-house gene ontology database to annotate the molecular functions of all identified HS-responsive genes. Third, to determine which sequences are conserved in the promoters of HS-inducible genes, we analyzed all hexamer sequences using our promoter research tool. Fourth, based on detailed bioinformatics predictions of conserved sequences, we attempted to design a HS-specific inducible promoter and then performed functional analyses of the designed promoter. The synthetic HSE was placed in an optimal position of promoter, followed by a β-glucuronidase reporter gene (*GUS*). In our functional analyses, transcript levels of marker genes were significantly higher in cold-, dehydration-, or ABA-treated transgenic plants than in untreated transgenic plants. GUS expression did not increase in each stress-treated transgenic plant; however, its expression increased significantly in HS-treated transgenic plants (Figure 1). We also performed in vivo single-cell gene induction using an infrared laser-evoked gene operator (IR-LEGO) system to observe GUS activity in irradiated cells (Figure 2). These findings demonstrate the utility of our HS-inducible promoter, which we expect to contribute to future molecular breeding of plants adapted to climate change and for the in vivo analysis of gene functions when gene expression is controlled by spatial and/or temporal conditions.

(*K. Maruyama, T. Ogata, N. Kanamori, S. Goto [NARO], Y.Y. Yamamoto [Gifu University], H. Urawa [Gifu Shotoku Gakuen University], S. Iuchi, K. Urano, T. Sakurai, H. Sakakibara, K. Shinozaki [RIKEN], K. Yamaguchi-Shinozaki [The University of Tokyo]*)

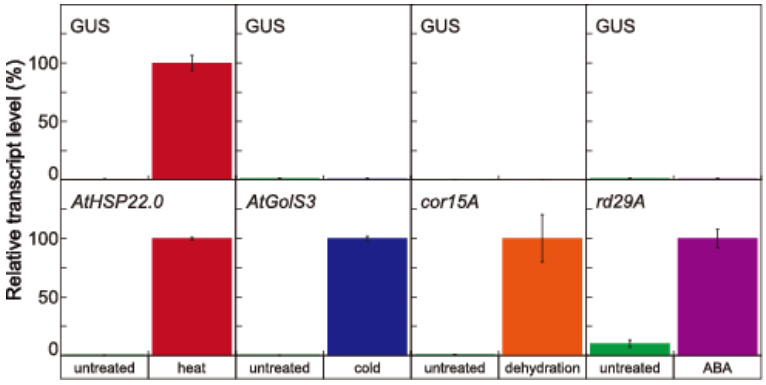

Fig. 1. Transcriptional activity of the optimal HS-inducible synthetic promoter. Levels of transcripts for genes encoding β-glucuronidase reporter gene (*GUS*) and condition-specific markers (heat, *AtHSP22.0*; cold, *AtGols3*; dehydration, *cor15A*; and ABA, *rd29A*) by quantitative reverse transcription (qRT)-PCR in transgenic plants.

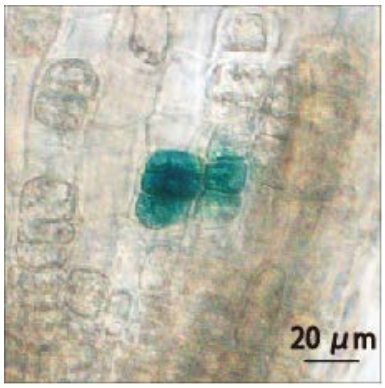

Fig. 2. GUS expression induced by infrared laser irradiation of target cells in *Arabidopsis* lateral root tips. We performed in vivo single-cell gene induction using an infrared laser-evoked gene operator (IR-LEGO) system to observe GUS activity in irradiated cells.

B-03

Draft genome sequence of an inbred line of *Chenopodium quinoa*, an allotetraploid pseudocereal crop with high nutritional properties and tolerance to abiotic stresses

Chenopodium quinoa (quinoa) is an annual herbaceous plant that originated from the Andes region of South America. It is a pseudocereal crop of the Amaranthaceae family, which also includes spinach (*Spinacia oleracea*) and sugar beet (*Beta vulgaris*). Quinoa is emerging as a key crop with the potential to contribute to global food security, and is considered to be an optimal food source for astronauts due to its great nutritional profile and ability to tolerate adverse environments such as high salinity. In addition, plant virologists utilize quinoa as a representative diagnostic host to identify virus species.

The major cultivation area of quinoa ranges from Columbia to central Chile, and includes altitudes from 0 m up to 4,000 m above sea level receiving an annual amount of rainfall of 80mm to 2,000mm. Quinoa exhibits great tolerance to soil salinity, frost, and drought, thus it is well suited for growing under unfavorable climatic and environmental conditions and. Moreover, quinoa is an excellent nutritional source of various minerals (e.g., Ca, Fe, P, and Zn), vitamins (e.g., A, B1, B2, C, and E), linolenate, natural antioxidants such as polyphenols, dietary fiber, and high-quality protein containing high levels of essential amino acids. Being gluten-free, quinoa is suitable for consumption by individuals who are allergic or intolerant to wheat, rye, and barley. Because of the great nutritional value of quinoa seeds and the high adaptability of quinoa plants to hostile environments, quinoa is deemed by the Food and Agriculture Organization of the United Nations (FAO) to be an important crop with the potential to contribute to food security worldwide. Moreover, the USA's National Aeronautics and Space Administration (NASA) considers quinoa as an optimal food source for astronauts on long-term space missions in isolated conditions. However, molecular analysis of quinoa is restricted by its genome complexity derived from allotetraploidy and its genetic heterogeneity due to outcrossing.

To overcome these limitations, we established the inbred and standard quinoa accession Kd that allows molecular analysis to unravel the mechanism of its high nutritional value, tolerance to unfavourable environments, and susceptibility to a broad range of viruses, and provided the draft genome sequence of Kd using an optimized combination of high-throughput next generation sequencing on the PacBio RS II and Illumina Hiseq 2500 sequencers. The *de novo* genome assembly contained 25 k scaffolds consisting of 1 Gbp with N50 length of 86 kbp. Based on these data, we constructed the free-access Quinoa Genome DataBase (QGDB; http://quinoa.kazusa.or.jp), which provides annotations of *in silico* predicted genes. Furthermore, we utilized comparative genomics and experimental approaches to identify genes in quinoa that are involved in abiotic and biotic stress responses. Thus, these findings yield insights into the effect of allotetraploidy on genome evolution and the mechanisms underlying agronomically important traits of quinoa.

(Y. Fujita, Y. Yasui [Kyoto University], H. Hirakawa [Kazusa DNA Research Institute], M. Mori [Ishikawa Prefectural University], T. Tanaka [Actree Co.])

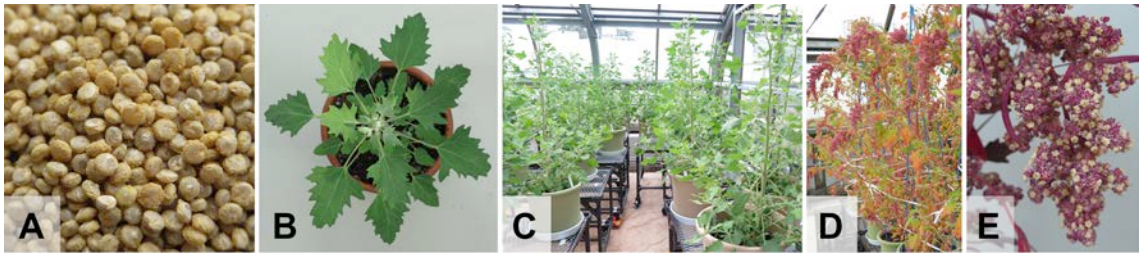

Fig. 1. Morphological characteristics of quinoa (Kd) plants. (A) Dried mature quinoa (Kd) seeds. (B, C, D) 6-, 8-, and 16-week-old quinoa (Kd) plants grown in soil. (E) Head of 17-week-old quinoa plants at harvest time.

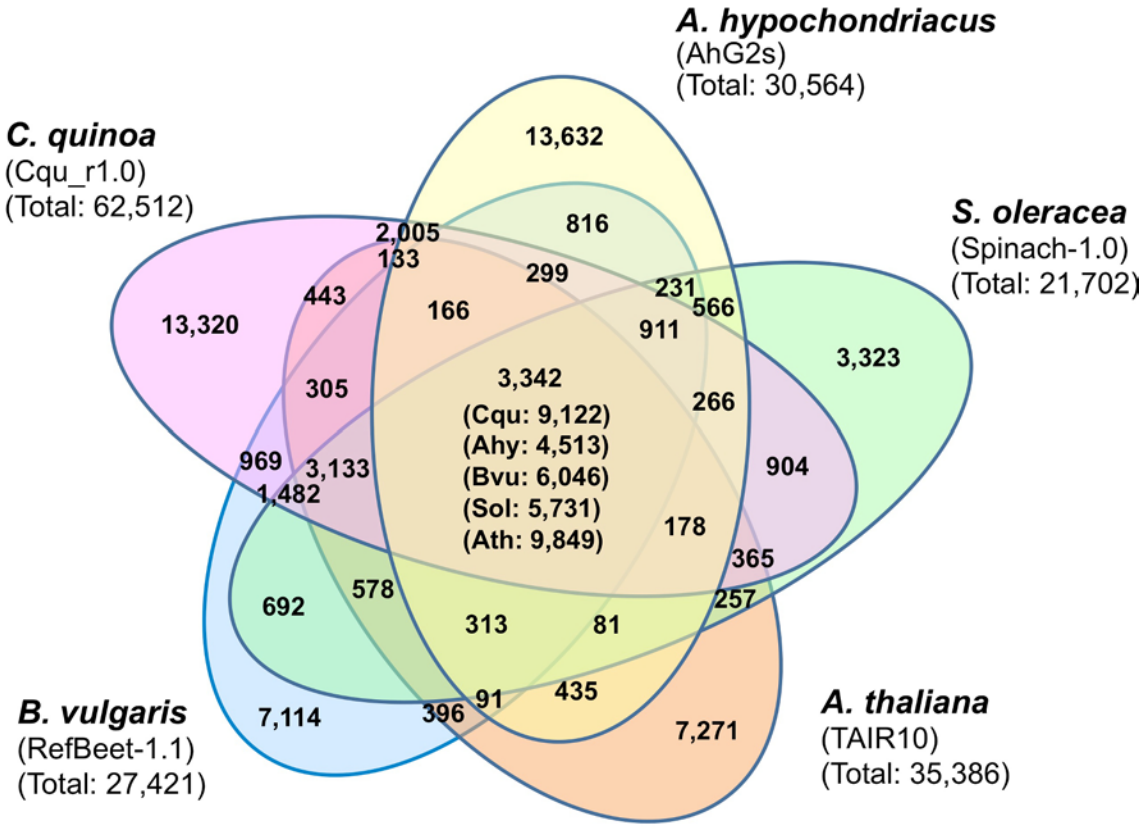

Fig. 2. Cluster analysis of the 62,512 filtered gene sequences. Predicted genes in *Chenopodeum quinoa*, *Amaranthus hypochondriacus*, *Beta vulgaris*, *Spinacia oleracea*, and *Arabidopsis thaliana* were clustered into gene families. In this analysis, we used the filtered dataset of quinoa consisting of 62,512 sequences annotated by performing BLASTP searches against the NCBI's NR database. The number in each section represents the number of clusters, and the numbers in parentheses in the center section represent the numbers of genes included in the analysis from each species. The number below the species name marks the total number of genes used as input for CD-hit (-c 0.4, -aL: 0.4).

Enhancement of ozone resistance by adjusting the stomatal aperture on leaf surface

Tropospheric ozone (O_3) is a major photochemical oxidant and one of the most phytotoxic air pollutants. Ozone levels have been increasing in many parts of the world, with high concentrations of ozone causing serious damage to crop production. Because ozone enters the plant through the stomata, modulation of stomatal movement using transcription factors, which act as master regulators of various cellular processes, may be a useful strategy for conferring ozone resistance. However, transcription factors modulating stomatal movement have not been well characterized.

In this report, we screened a set of transgenic *Arabidopsis* lines expressing chimeric repressors for *Arabidopsis* transcription factors to identify new transcription factors related with ozone stress resistance. We found that lines expressing the chimeric repressors for GOLDEN 2-LIKE1 (GLK1) and GLK2, which have known functions in chloroplast development, exhibit remarkable ozone resistance and a closed-stomata phenotype. In addition to ozone resistance, these plants also exhibited resistance to sulfur dioxide, an oxidative stress reagent similar to ozone. On the other hand, plants that overexpress GLK1/2 exhibited higher sensitivity to ozone and sulfur dioxide, and an open-stomata phenotype. These results suggest that GLK1/2 affect ozone and sulfur dioxide resistance through the regulation of stomatal movement. We showed that lines expressing the chimeric repressors for GLK1 had reduced expression of the genes for inwardly rectifying K^+ (K^+_{in}) channels and reduced K^+_{in} channel activity, which is one of the positive regulators for stomatal opening. These results indicate that GLK1/2 act as positive regulators of genes for K^+_{in} channels and stomatal opening.

Stomata play roles in the transpiration and absorption of gases in plants. Thus, the modification of stomatal movements could prove useful for improving both the efficiency of photosynthesis and the plants' resistance to air pollutants. Regulating the expression of chimeric repressors for GLK1/2 specifically in guard cells may be a useful tool for conferring resistance to air pollutants.

(Y. Nagatoshi, N. Mitsuda [National Institute of Advanced Industrial Science and Technology], M. Hayashi [Nagoya University], S. Inoue [Nagoya University], E. Okuma [Okayama University], A. Kubo [National Institute for Environmental Studies], Y. Murata [Okayama University], M. Seo [RIKEN Center for Sustainable Resource Science], H. Saji [National Institute for Environmental Studies], T. Kinoshita [Nagoya University], M. Takagi [Saitama University])

Fig. 1. Sensitivity to ozone of GLK1/2-downregulated *Arabidopsis*.

A. Two-week-old plants of wild type and GLK1/2-downregulated *Arabidopsis* (*GLK1sx* and *GLK2sx*) 1d after exposure to 0.3 ppm ozone for 7h.

B. Ion leakage of wild type and *GLK1/2sx* plants. The average of three biological replicates (three plants per replicate) is shown. Error bars represent SD.

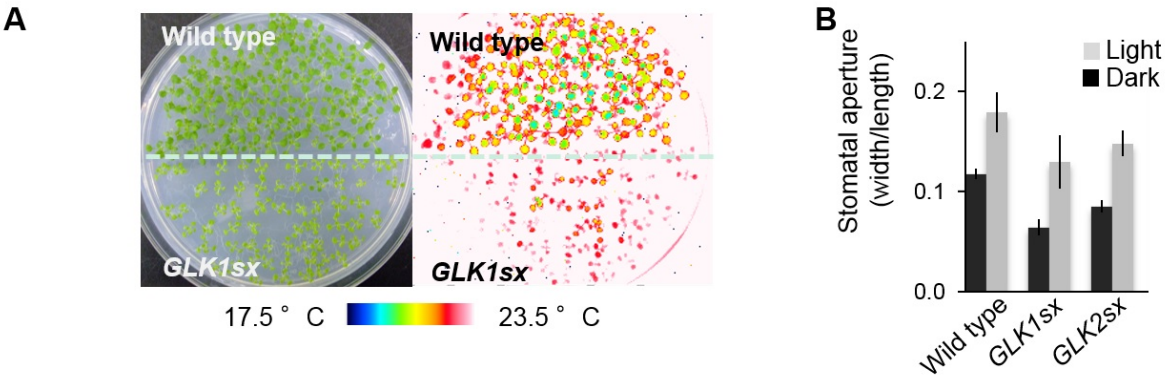

Fig. 2. Transpiration and stomatal aperture of GLK1/2-downregulated *Arabidopsis*.

A. Thermal images of wild type and *GLK1sx* plants grown on MS medium, showing the higher temperature of *GLK1sx* plants.

B. Stomatal aperture of wild type and *GLK1sx* plants grown on MS medium. The average of three independent experiments is shown (50 stomata per experiment).
Error bars represent SD.

Genome editing systems in rice cultivars and strategy for producing desired mutants with homozygous mutation

CRISPR/Cas9 is a novel tool for targeted mutagenesis and is applicable to plants, including rice. The reported studies used limited rice cultivars that have high transformation efficiencies but are now used only for research purposes. For practical application of genome editing to molecular breeding in rice, there is a need to establish CRISPR/Cas9 systems that can be used in commercial cultivars. In targeted mutagenesis, biallelic homozygous mutants in which the target mutations are inherited stably by later generations are desirable for molecular breeding. Previous reports on CRISPR/Cas9 in rice have demonstrated that target mutations are transmitted to the next generation in accordance with Mendelian law, but heritability of the target mutation and the role of inherited *Cas9* gene have not been fully elucidated. Here, we targeted the rice phytoene desaturase (*OsPDS*), whose mutants exhibit an albino phenotype, in five rice cultivars by using CRISPR/Cas9 and analyzed the segregation of target mutations. We present a strategy for generating homozygous mutants without transgenes, chimerism, or unpredicted mutations by using CRISPR/Cas9 in rice.

Agrobacterium-mediated methods using immature embryos successfully transformed a CRISPR/Cas9 system into five rice cultivars including commercially important ones and subsequently induced mutation (Table 1). Unpredicted segregations, with more mutants than theoretically predicted, were frequently found in T_1 plants from monoallelic T_0 mutants. Chimeric plants with both biallelic and monoallelic mutated cells were also observed in the T_1 (Fig. 1). Next, we followed the segregation of a target mutation in the T_2 from monoallelic T_1 mutants. When T_1 mutants possessed *Cas9*, unpredicted segregations of the target mutation and chimeric plants were observed again in the T_2. When T_1 mutants did not possess *Cas9*, segregation of the target mutations followed Mendelian law and no chimeric plants appeared in the T_2. T_2 mutants with *Cas9* had mutations different from the original ones found in T_0. Our results indicated that inherited *Cas9* was still active in later generations and could induce new mutations in the progeny, leading to chimerism and unpredicted segregation (Fig. 2). We conclude that *Cas9* must be eliminated by segregation in T_1 to generate homozygous mutants without chimerism or unpredicted segregation.

Genes of commercially important rice cultivars can be modified by using CRISPR/Cas9 through our transformation systems, as has been done for other “model” cultivars. Investigators also must consider the possibility of unpredicted segregation caused by somatic mutation in T_0, off-target mutagenesis, and somaclonal variation, which usually can occur in CRISPR/Cas9 technologies. For the practical use of mutants produced by our systems, intellectual property rights must be handled accordingly.

(T. Ishizaki)

Table 1. Genotypes of rice cultivar mutants of *OsPDS*, produced by using the CRISPR/Cas9 system and by *Agrobacterium*-mediated transformation of immature embryos.

Cultivar	Number of transgenic plants	Number of monoallelic mutants	Number of biallelic mutants	Total number of mutants
Nipponbare	106	26	64	90
Koshihikari	17	1	10	11
NERICA1	54	16	33	49
Curinga	272	137	80	217
IR64	5	4	1	5
Total	454	184	188	372

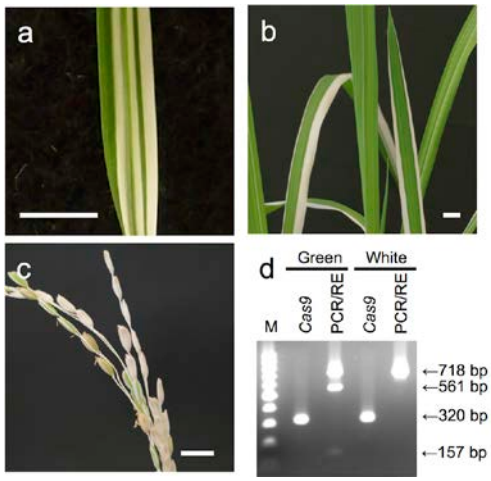

Fig. 1. Segregation of chimeric plants in the T_1. (a) Leaf of chimeric plant at seedling stage. (b) Leaves of chimeric plants grown in a greenhouse. (c) Spikelet of a chimeric plant. Bars represent 1 cm. (d) Green and white portions of chimeric plants were separately subjected to PCR-RE assay for *OsPDS* and to PCR assay for *Cas9*. In the case of monoallelic mutants, PCR-RE assay indicated three bands: 718 bp, 320 bp and 157 bp. In the case of biallelic mutants, PCR-RE assay indicated only a single band: 718 bp. Expected size of PCR products of *Cas9* was 320 bp.

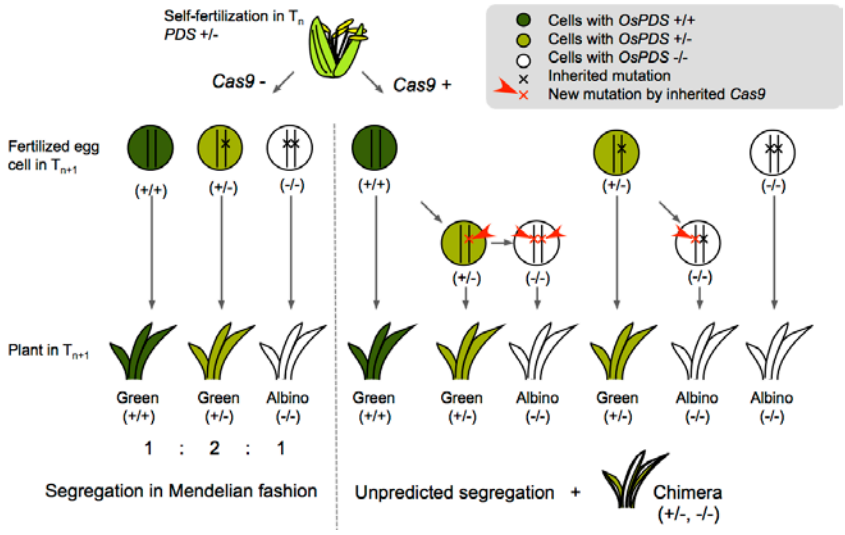

Fig. 2. Diagrammatic model of unpredicted segregation. When plants do not inherit *Cas9*, the targeted mutation segregates in a Mendelian fashion. When plants inherit *Cas9*, the *Cas9* can induce new mutations leading to unpredicted segregation and chimerism.

B-06

Three differential soybean varieties highly resistant to Asian soybean rust carry the resistance gene *Rpp1-b*

Asian soybean rust (ASR), a soybean disease caused by *Phakopsora pachyrhizi*, is one of the biggest threats to soybean production in South America where more than half of soybean in the world market is produced. Although an environment-friendly, cost-effective, and long-term management of ASR can be achieved through use of ASR-resistant soybean cultivars, only a limited number of resistance resources are available for soybean breeding in South America because of the high virulence and diversity of ASR pathogens. For this reason, we are examining ASR-resistant soybeans whose resistance genes have not been identified yet and are therefore unused in breeding programs. We previously studied the Chinese soybean varieties PI 594767A (Zhao Ping Hei Dou), PI 587905 (Xiao Huang Dou), PI 587855 (Jia Bai Jia), and Xiao Jin Huang, and the Japanese soybean varieties Himeshirazu, Iyodaizu B, and PI 416764 (Akasaya). We identified their resistance to ASR pathogens from South America and Japan, with PI 594767A, PI 587905, PI 587855, and PI 416764 among those included in the international set of soybean differentials used in identifying the pathogenicity of ASR pathogens. The aim of this study, therefore, was to identify the ASR-resistance loci in these seven soybean varieties and tag the resistance genes to DNA markers. This information will be useful in marker-assisted breeding programs for ASR resistance.

F_2 populations were developed by crossing a susceptible variety, BRS184, with each of the seven resistant varieties. Each population was inoculated with an appropriate ASR pathogen and the phenotypes were determined as either resistant (R) or susceptible (S). Then, the loci for ASR resistance were mapped together with the DNA markers. In case the boundary between R and S was unclear in the F_2 population, the resistance locus was mapped as a quantitative trait locus (QTL) for sporulation level (SL).

Figure 1 shows that Xiao Jin Huang and Himeshirazu carry *Rpp1*, whereas PI 594767A, PI 587905, and PI 587855 carry *Rpp1-b*. *Rpp1* and *Rpp1-b*, both known as ASR-resistance genes, are located close to each other on chromosome 18. Furthermore, the QTL for SL was mapped on the chromosome region of *Rpp2* and *Rpp3* for Iyodaizu B and PI 416764, respectively. Since the ASR resistance loci of these seven soybean varieties were successfully identified together with the DNA markers linked to their resistance loci, these resistant varieties can be used in marker-assisted breeding programs for ASR resistance. Among the seven varieties, PI 594767A, PI 587905, and PI 587855 have been found to carry *Rpp1-b*. They are especially useful for soybean breeding because they are resistant not only to 78.6%-96.5% of ASR pathogens from South America and Japan but also to three highly virulent Brazilian ASR races (Table 1).

(N. Yamanaka, M. M. Hossain [Bangabandhu Sheikh Mujibur Rahman Agricultural University])

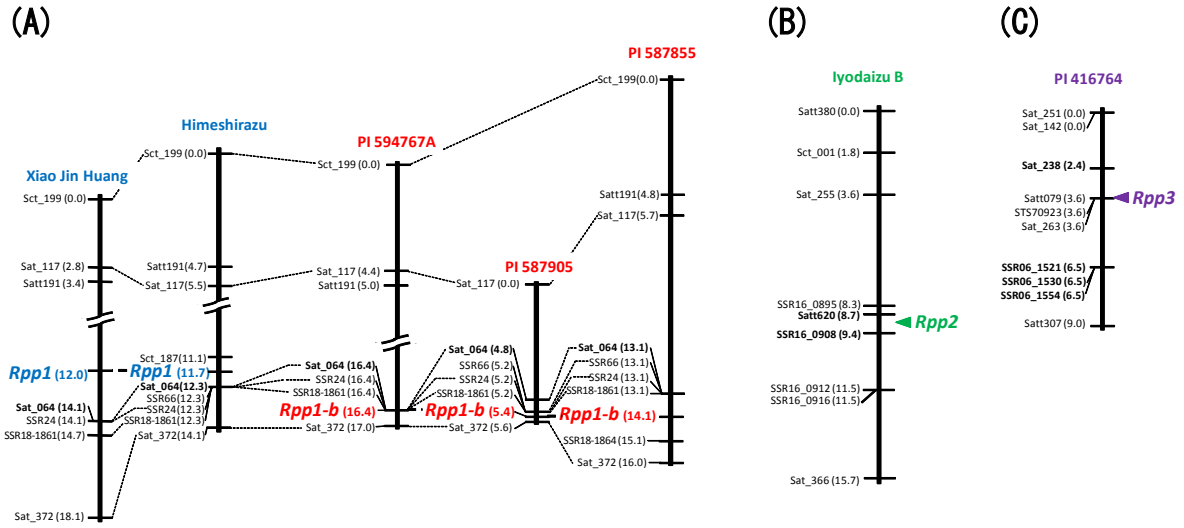

Fig. 1. Molecular linkage maps of ASR resistance loci in seven soybean varieties. It shows (A) soybean chromosome 18 where *Rpp1* and *Rpp1-b* are located; (B) chromosome 16 where *Rpp2* is located; and (C) chromosome 6 where *Rpp3* is located. The loci *Rpp2* and *Rpp3* were determined by quantitative trait locus (QTL) analysis for sporulation level (SL) in ASR disease. The names of DNA markers and genetic distance (cM) from the top of linkage groups are shown on the left side of each linkage group.

Table 1. Reactions of seven ASR-resistance soybean varieties to ASR pathogens from South America and Japan

Soybean variety	Gene	Highly virulent Brazilian ASR pathogen				Japanese ASR pathogen		Frequency of resistant phenotype to 64 pathogens from South America and Japan
		BRP-2.49	BRP-2.1	BRP-2.6	BRP-2.5	T1-2	E1-4-12	
Xiao Jin Huang	*Rpp1*	S	S	S	S	R	SR	9.7 - 16.1%*
Himeshirazu	*Rpp1*	S	S	S	S	S	HR	9.7 - 16.1%*
PI 594767A	*Rpp1-b*	HR	HR	HR	S	HR	HR	96.5%
PI 587905	*Rpp1-b*	HR	HR	R	S	R	HR	84.1%
PI 587855	*Rpp1-b*	HR	R	HR	S	-	HR	78.6%
Iyodaizu B	*Rpp2*	R	SR	S	S	S	HR	25.8 - 31.8%*
PI 416764	*Rpp3*	S	S	S	S	R	HR	34.4%

HR: Highly resistant; R: Resistant; SR: Slightly resistant; S: Susceptible; -: No data.

*The ranges of frequencies shown here are based on different varieties but carrying either *Rpp1* or *Rpp2*.

C-01

Selective protein digestion during fermentation provides a distinctive texture to traditional fermented rice noodles in Indochina

Traditional fermented rice noodles in Indochina are characterized by their unique flavor and pleasing texture. Locally known as Kanom-jeen (Thailand), Khao Pun (Laos), and Bun (Vietnam), they are widely consumed as a staple food throughout the region with the fermentation process considered a key step in providing its desirable attributes, especially texture.

Traditional preparation of Thai traditional fermented rice noodles, Kanom-jeen, involves the following steps: soaking of high amylose rice for 4-5 h in water, fermentation of the soaked rice grains for 3 days with aeration, wet-milling, fermentation of ground flour in saline solution for 3 days, filtration, kneading and pre-gelatinization, re-kneading to form a viscous slurry, extruding the viscous slurry into noodles, and cooking in boiling water (Fig. 1).

The results showed that protein content significantly decreased during the 1st aerobic fermentation process for 3 days as shown in Figure 2. Their protein composition revealed that Protein Body II, the digestible proteins in rice kernel, disappeared during rice fermentation, while Protein Body I, the indigestible proteins, remained. Microstructural analysis (Fig. 3) demonstrated that cluster-like structures consisting of digestible proteins were formed only in the non-fermented preparation, while fermented preparation contained only uniformly spherical protein bodies formed by the indigestible proteins in starch gel. The cluster-like protein structures are commonly found in gels of non-fermented noodles, resulting in a less uniform microstructure. These structural differences indicated that the traditional fermentation process can be considered a viable method for removing digestible proteins selectively from rice endosperm to provide a stronger gel. The fermentation process is, therefore, necessary during preparation to obtain the desired specific texture.

Eliminated proteins can be identified as part of rice allergenic proteins. Therefore, these findings may shed light on the effect of traditional processes on selective digestibility to determine its potential to reduce rice allergenicity. Moreover, remaining proteins that are indigestible have been considered as beneficial for chronic kidney disease patients who need to control their protein intake. These properties could provide benefits as a healthy food application based on traditional processing knowledge, consequently increasing the nutritional value of local traditional products.

(P. Satmalee [Institute of Food Research and Product Development, Kasetsart University (IFRPD, KU)], V. Surojanametakul [IFRPD, KU], N. Phomkaivorn [IFRPD, KU], W. Pantavee [IFRPD, KU], T. Yoshihashi)

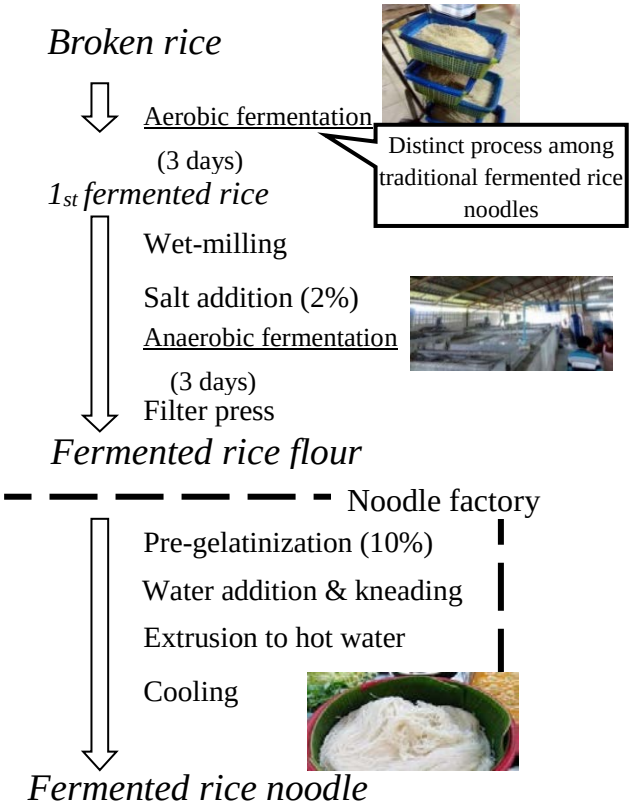

Fig. 1. Traditional processing of Thai fermented rice noodles, Kanom-jeen.

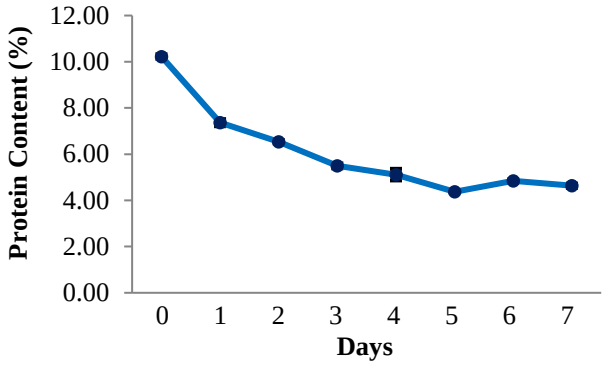

Fig. 2. Changes in protein content of rice during fermentation.
Protein content significantly decreased during the 1st aerobic fermentation process for 3 days.

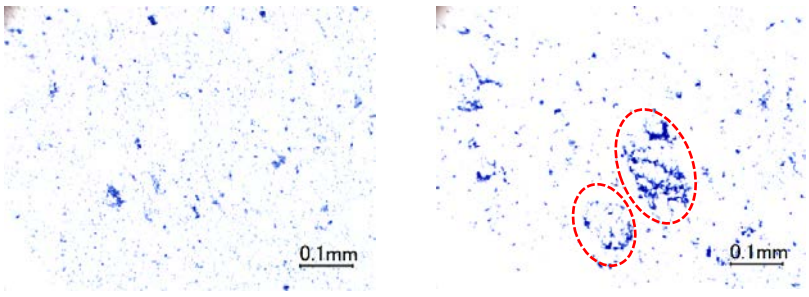

(a) (b)

Fig. 3. Protein localization in fermented (a) and non-fermented (b) rice noodles.
Cluster-like structures of digestible proteins were observed only in non-fermented noodles.

C-02

Effect of cassava pulp supplement on 1,3-propanediol production by *Clostridium butyricum*

The three-carbon diol 1,3-propanediol (1, 3-PD) is an important organic substrate for biopolymers such as polytrimethylene terephthalate. Glycerol, which is a by-product of biodiesel production, is the main substrate of 1,3-PD production by fermentation with microorganisms such as *Clostridium butyricum*. However, the yield and productivity of 1,3-PD on glycerol are low because the growth and energy production are hampered by the low assimilation rate. Supplementing the glycerol medium with glucose is expected to enhance the growth and increase of 1,3-PD production; however, it leads to catabolite repression in *C. butyricum*. Although *C. butyricum* can produce solvents from polysaccharides such as starch, the effects of polysaccharides on 1,3-PD production by this organism have not been reported. We report that supplementing the glycerol medium with small amounts of cassava pulp (CP) rather than starchy polysaccharides can improve the 1,3-PD productivity of *C. butyricum*. CP is a promising starchy-lignocellulosic biomass for biochemical production because both of its major components, namely, starch (50% dry basis) and cellulose fiber (approximately 30% dry basis), can be hydrolyzed to fermentable sugars. When the medium containing 30 g/L glycerol was supplemented with 2 g/L and 4 g/L CP (1 g/L and 2 g/L starch, respectively), the 1,3-PD concentrations were 9.5 g/L and 8.2 g/L, respectively, similar to that of glycerol alone. However, CP supplementation increased the rate of 1,3-PD production by *C. butyricum*. Specifically, in a medium containing 30 g/L of glycerol supplemented with 2 g/L of CP, the productivity of 1,3-PD (g/L/h) after 24 hours of fermentation was enhanced from 0.25 ± 0.01 (in 30 g/L of glycerol alone) to 0.43 ± 0.02. These results indicate that supplementation with small quantities of CP not only improves the poor growth of *C. butyricum* on glycerol medium but might also enhance 1,3-PD production by this organism.

(W. Apiwatanapiwat [Kasetsart University], P. Vaithanomsat [Kasetsart University], A. Kosugi)

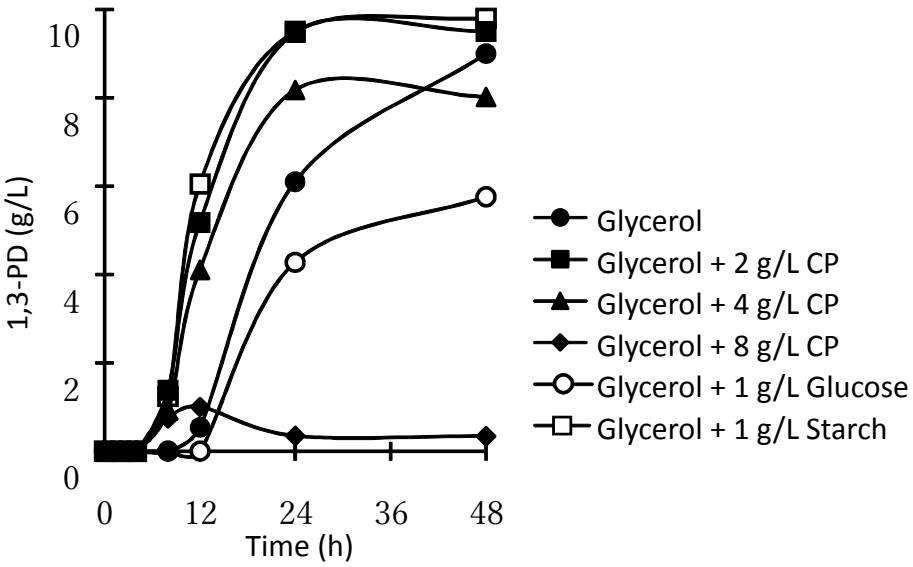

Fig. 1. Profiles of fermentative 1,3-PD production by *C. butyricum* I5-42 during batch fermentation on medium (containing 30 g/L glycerol) supplemented with CP at various concentrations.

C-03

Resource management and conservation of *Pa koh*, an important edible fish in Laos, based on ecological information

Laos has been experiencing a high population growth rate in recent years, resulting to the expansion of urban areas and a rapid increase in demand for edible fish. This has become a serious concern as it has led to a declining stock level of many fish species and a downsizing of the specimens. The snakehead fish, locally called *Pa koh* (*Channa striata*) (Fig. 1), is among those facing strong fishing pressure because of its daintiness and high market value. This species is strongly carnivorous, has a superior position in the regional food chain, and its population size is relatively small compared to other non-carnivorous fishes. This situation necessitates stock management of the species and require conservation of the adult specimens (breeding population).

Against this background, an analysis of several ecological features such as age, growth, and reproduction were carried out in the present study using 530 specimens collected from the northern area of Vientiane Province, Laos, and the following findings relevant to efficient stock management were obtained.

1. In the otoliths of *Pa koh*, a translucent zone is formed once per year and a ring structure is deposited (Fig. 1). This ring is an annual ring and it is useful for estimating the ages of each specimen.
2. By counting the number of annual rings, the growth models (age–size relationships) are regressed, and the reproductive age and longevity can be estimated. The maximum age and size observed in the present study are 6–7 years old and approximately 50 cm standard length (SL), respectively, for both females and males (Fig. 2).
3. The growth patterns of females and males are not significantly different from the growth models (von Bertalanffy growth curves) (Fig. 2), and the model indicates slower growth compared to the growth of *C. striata* studied in other tropical areas (e.g., Sri Lanka).
4. On the basis of the growth model, gonad somatic index (GSI, gonad weight / body weight × 100 %), and size-GSI relationship (figure omitted), this species was found to sexually mature at approximately 20 cm SL (2 years old). Ovary maturation progresses from the late phase of the dry season (March) as the water temperature rises, the peak of reproduction being in April (Fig. 3).
5. In order to manage / conserve *Pa koh* stock, fishing restriction on specimens larger than 20 cm SL during breeding period (from April to June) must be imposed. Setting a non-fishing period and/or non-fishing area(s) in breeding area(s) is considered efficient.

In addition to the above findings, the following observations were noted.

1. Since several populations of *Pa koh* are widely distributed over Laos, further investigations on other populations in other areas are required for stock management in more widespread areas.
2. Juveniles of *Pa koh* (4-5 cm SL) abundantly occur in the shallow area(s) of ponds/lakes/rivers, and they are also caught as edible food. It is also necessary that such activity be controlled for better stock management of *Pa koh*.

(S. Morioka, B. Vongvichith [Living Aquatic Resources Research Center])

C-03

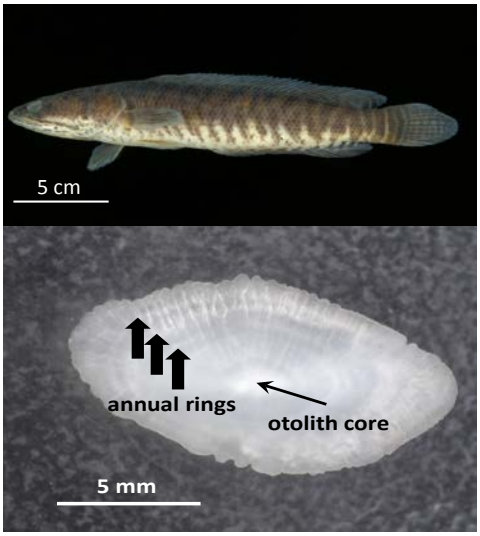

Fig. 1. Top: An adult *Pa koh* (24 cm SL); Bottom: Otolith and annual rings

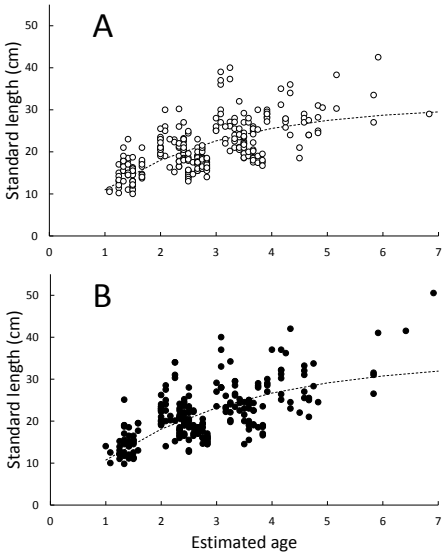

Fig. 2. Growth models of *Pa koh* (A: female; B: male)

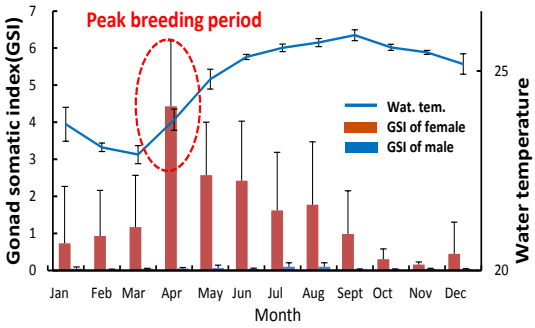

Fig. 3. Seasonal changes in the GSI of *Pa koh* and in water temperature.

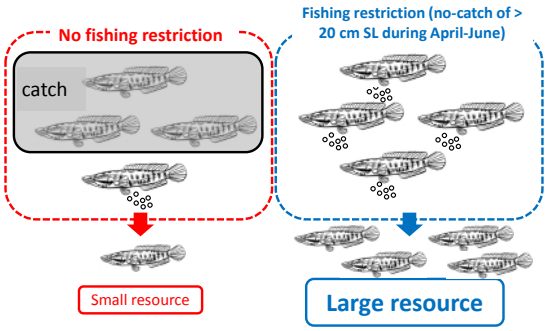

Fig. 4. Images showing the effects of unrestricted and restricted fishing

C-04

Improvement of selective logging criteria for dipterocarp timber species to maintain healthy seed production

Maintaining regeneration is essential for sustainable forest management when products, such as timber, are being extracted. It has been widely believed that the forests have sufficient resilience to recover from selective logging without enrichment planting, and selective logging regimes have been widely applied in sustainable management programs for tropical forests. However, selective logging may also threaten the pollination and sexual reproduction systems of tropical tree species. Consequently, outcrossing restrictions can markedly increase the proportion of unhealthy offspring through inbreeding depression. Thus, selective logging regimes must be optimized in terms of remaining tree density to ensure that healthy outcrossed seeds are produced in sufficient numbers to support the sustainable management of secondary forests.

Parameters of pollen dispersal and flowering intensity were estimated from paternity of seeds collected from mother trees of four focal dipterocarp timber species and a subsequent hierarchical Bayesian model (See JIRCAS Research Highlights 2011, Topic 15). To simulate reductions in outcrossing pollen clouds after logging, we raised the selective logging criterion (cutting limit) in 1 cm increments from 40 cm to 100 cm. At each step, we calculated the amount of outcrossing pollen in the pollen cloud of the mother trees from the remnant trees which were smaller than the arbitrarily assigned cutting limit. However, we applied unified parameter values for every simulation step.

Pollen dispersal patterns of dipterocarps are strongly affected by population density. Thus, as logging inevitably affects population density, it is not realistic to apply the same pollen dispersal kernel parameter estimates following logging at every cutting limit applied in simulations. The unrealistic feature of the simulation should be carefully considered before applying the results in practice. It is still a useful tool to gauge how the reduction in population densities and outcrossing pollen clouds may affect the proportion of healthy outcrossed seeds in selectively logged forests.

The simulation results presented here clearly indicate that outcrossing of *S. curtisii* is most susceptible, with *S. maxwelliana* being second most susceptible, to reductions in population density due to selective logging among the four focal dipterocarp species (Fig. 1). These species produce highly durable timber, which could relate to species' turnover rates, as species with high wood densities have low growth rates, low susceptibility to forest disturbance, and low mortality rates. In addition, the onset of reproduction at relatively large sizes for the species may increase the vulnerability of the pollen dispersal to reduction of population density due to selective logging. The post-logging decline in male fecundity in the remaining small-sized trees as implied in the simulations for *S. maxwelliana* and *S. curtisii*, which have highly dense wood, underscores the need for more species-specific cutting guidelines (Table 1). Based on our study, defining groups of timber species according to their wood density could facilitate efforts to formulate selective logging schemes that better balance the exploitation and genetic conservation of dipterocarp timber species.

C-04

(N. Tani, S.L. Lee [Forest Research Institute Malaysia], C.T. Lee [FRIM], K.K.S. Ng [FRIM], N. Muhammad [FRIM], A.R. Kassim [FRIM], S. Musa [FRIM], Y. Tsumura [University of Tsukuba])

Table 1. Ecological difference between the experimental timber species and improvement plan in response to the simulation results

Timber species		Ecological feature				Healthy seed production	
Classification	Example	Wood density	Growth	Reproductive age	Longevity	Current criteria	Improvement plan
Fast-growing sp.	*S. leprosula* *S. parvifolia*	Low	Fast	Fast	Short	Healthy mating	Current criteria
Slow-growing sp.	*S. curtisii* *S. maxwelliana*	High	Slow	Slow	Long	Reducing healthy mating	More strict criteria

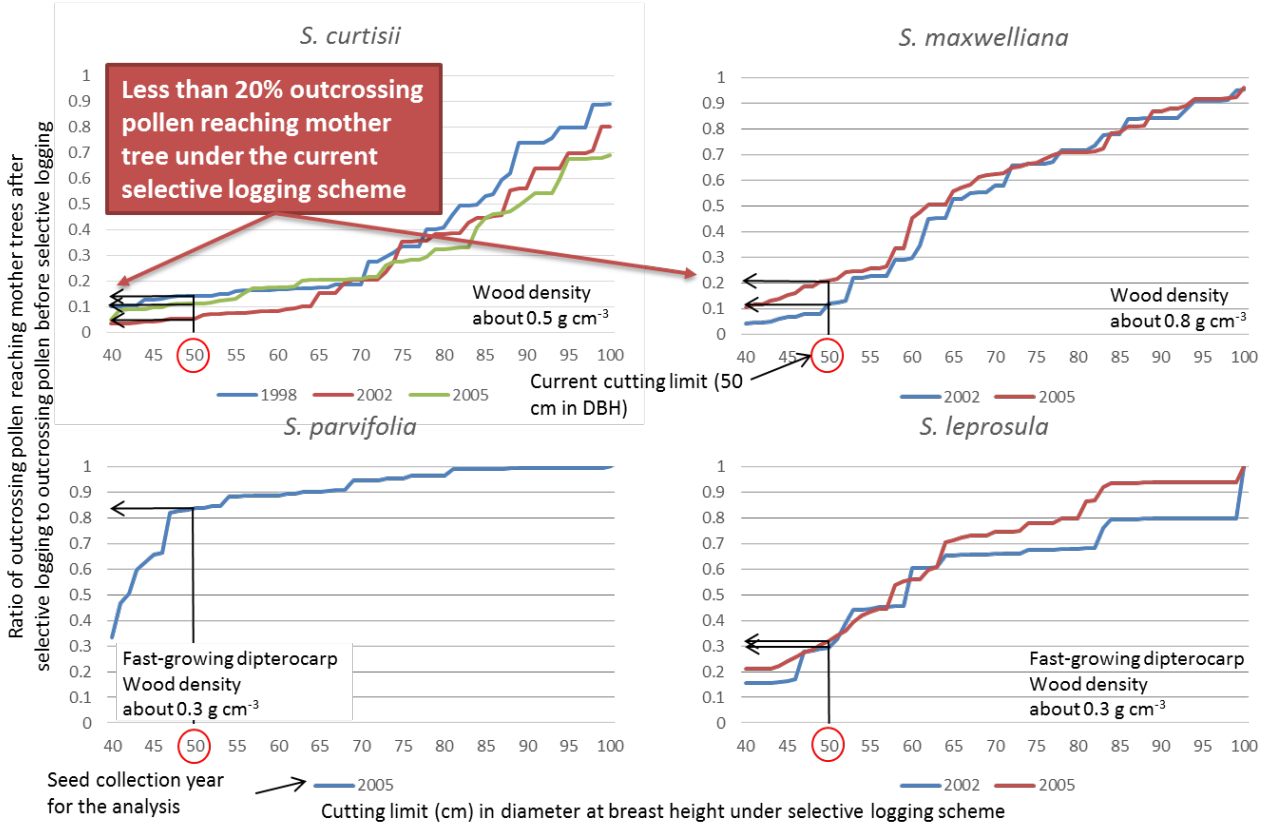

Fig. 1. Simulating the ratio of outcrossing pollen reaching mother trees after selective logging to outcrossing pollen without selective logging for four dipterocarp timber species. The simulation was conducted using the selective logging criterion (tree diameter cutting limit) of 40 cm and at every 1-cm increment thereafter.

C-05

Addition of charcoal to sandy soil in Northeast Thailand enhances growth of teak

Teak (*Tectona grandis* L. f.) is one of the most valuable timber tree species in Thailand, and it is widely planted throughout the country. However, teak growth in Northeast Thailand plantations is suppressed due to the low pH, low fertility, and low water holding capacity of the underlying sandy soil. Soil acidity can be corrected to raise the pH levels and fertilizers can be applied to improve the fertility of sandy soils, thereby accelerating the growth of teak. There have been previous researches on improving the water holding capacity of sandy soil, and some materials have been shown to be effective. However, these past studies did not examine the effect of these materials on the growth of teak.

In this study, we examined the availability of materials to improve the sandy soil's water holding capacity and increase teak growth. We selected bentonite (a clay consisting mostly of montmorillonite), charcoal, and corncob, and added these materials at the rate of 4% (by weight) to sandy soil in Northeast Thailand. The mixtures were put into 8.5-L pots, and teak seedlings were planted on these pots and raised for one year. We measured soil water content and leaf water potential at predawn. At the end of the experiment, we sampled the teak seedlings, measured the dry mass of each organ, and analyzed the concentration of nutrients in leaves. Lastly, we compared the parameters among bentonite, charcoal, corncob, and no addition (control) treatments.

Results showed that water content was high for the bentonite treatment throughout the whole period (Fig. 1). For the charcoal treatment, water content increased from September 2013. In contrast, the corncob treatment showed low water content compared with the three other treatments. The predawn leaf water potential did not decrease for bentonite and charcoal treatments (Fig. 2). Moreover, teak seedlings grown on bentonite- and charcoal-treated plots could uptake water from the soil during the whole period and did not suffer from drought stress.

Charcoal treatment showed significantly higher root dry mass compared with the other treatments despite no fertilization (Fig. 3). The concentrations of phosphorus and potassium in the leaves of teak seedlings were significantly higher for the charcoal treatment compared with the control treatment (Fig. 4). In contrast, bentonite treatment did not show high concentrations of nutrients in leaves.

Based on our experiment, we concluded that charcoal was the most suitable material among those tested and would be very useful for improving teak growth at the seedling stage in sandy soils in Northeast Thailand. Charcoal is commonly produced in various countries, and thus may be applied as soil improvement material to enhance the water holding capacity and uptake of phosphorus.

(M. Kayama, S. Nimpila [Royal Forest Department], S. Hongthong [RFD], W. Wichiennopparat [RFD], W. Himmapan [RFD], T. Vacharangkura [RFD], R. Yoneda [Forestry and Forest Products Research Institute], I. Noda [FFPRI])

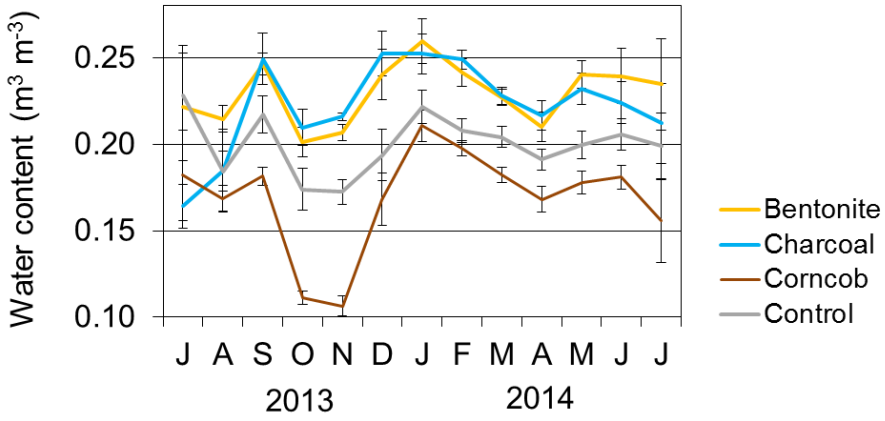

Fig. 1. Average soil water content before irrigation or rainfall (from July 2013 to July 2014)

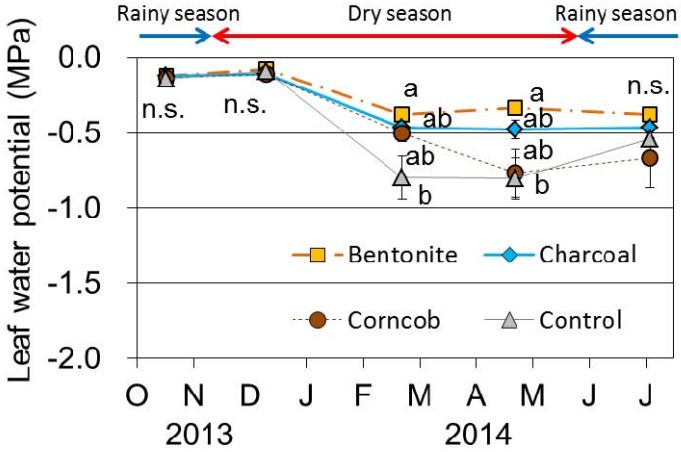

Fig. 2. Predawn leaf water potential of teak leaves (from October 2013 to July 2014)

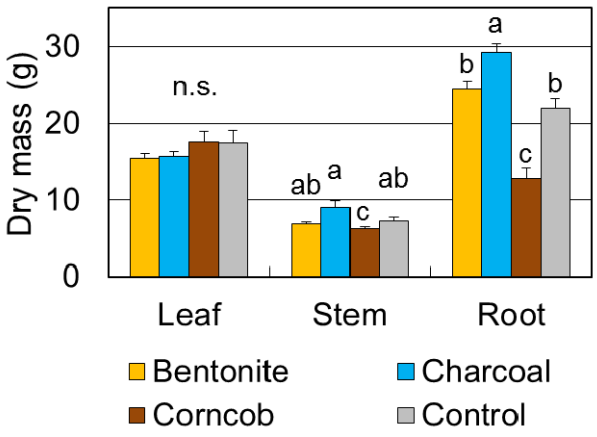

Fig. 3. Dry mass of each plant organ at the end of experiment (July 2014)

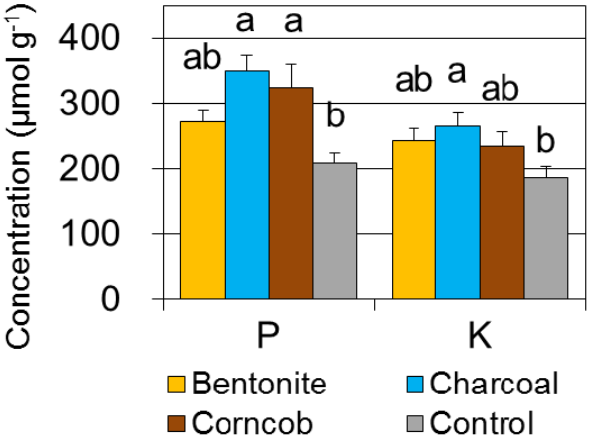

Fig. 4. Concentrations of phosphorus and potassium in teak leaves at the end of the experiment (July 2014)

C-06

Spread of infection of yellow head virus (YHV) of giant tiger prawns by cannibalism

Intensive Penaeidae cultivation is an important industry supporting the economy in tropical regions. However, due to recent disease outbreaks and their frequency (Fig. 1), the production in cultivation farms has become unstable and as such, a prompt solution is critical. In South-East Asia, yellow head virus (YHV) is a commonly occurring viral infection in shrimp. Since the first reports of YHV in Thailand, the virus continues to cause serious damage in various places. However, the transmission mechanism of the virus is still unclear. Shrimp farmers exchange the cultivation water as seldom as possible to avoid lateral infection which in turn results in water quality deterioration and reduced productivity. In this study, we carried out experiments in order to understand the mechanisms of YHV transmission and propose measures to reduce the impact of infections.

Amongst an experimental group allowed to cannibalize infected shrimp, more than 90% of all shrimp died from severe infection within 10 days (Fig. 2, Table 1). On the other hand, significantly lower rates of YHV detection and severity were identified amongst another group sharing the aquarium water with the cannibals but separated by a filter and the death rate was also significantly lower (Fig. 2, Table 1). Moreover, the YHV severity of shrimp in the second group that had survived low level infections gradually reduced after 30 days to 60 days (Table 1). These results show that YHV infection in shrimp is more severe if the infection was caused by cannibalism than by water. The gills from shrimp that had died from YHV were collected, homogenated, and filtered at 12 and 24 hours post-mortem respectively and injected into the muscle of healthy individuals. Those injected with gills collected 12 hours post death all died within 4 days. On the other hand, only one among those injected with gills collected 24 hours post death died after 7 days (Table 2). YHV activity is still high 12 hours post-mortem but significantly reduces after 24 hours. In shrimp cultivation, the possibility of YHV infection via pond water is low; therefore, avoiding water exchange is not necessary. Furthermore, it is more important to reduce the incidence of healthy individuals feeding (cannibalizing) on other shrimp that have died from YHV infection. For example, prompt collection of deceased individuals and low-density production would be effective measures against YHV infection.

Appropriate water exchange will enhance the water quality, which in turn will enhance the expected recovery of individuals with low level infections. Greater results could be anticipated by introducing and implementing specific pathogen-free (SPF) juvenile shrimp. The mechanism of the first occurrence of YHV infection in shrimp cultivation ponds is still unknown; hence, further studies are required for a detailed understanding of YHV infection.

(I. Tsutsui, K. Hamano [Japan Fisheries Research and Education Agency], D. Aue-um neoy [King Mongkut's Institute of Technology Ladkrabang])

Fig. 1. Giant tiger prawn infected with YHV at an earthen shrimp pond

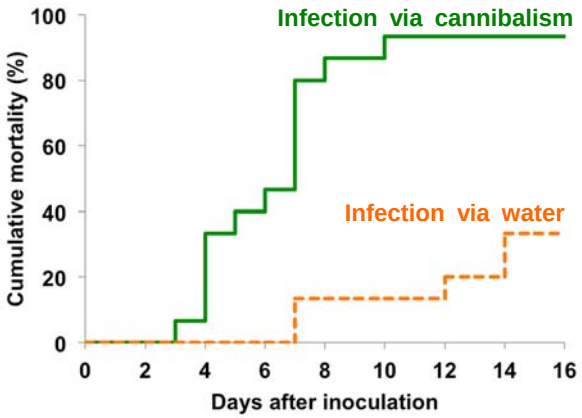

Fig. 2. Cumulative mortalities during a 16-day experiment between infected aquariums (through cannibalization and water borne routes)

Table 1. Number of deceased/surviving individuals and their infection intensity (infection through cannibalization and waterborne routes)

	Infection via cannibalism				Infection via water			
	Severely infected	Slightly infected	Undetectable	Total	Severely infected	Slightly infected	Undetectable	Total
Number of deaths	14	0	0	14	0	3	2	5
Survivors (30 days later)	0	0	1	1	0	5	5	10
(60 days later)	0	0	1	1	0	2	8	10

Deceased individuals were analyzed immediately post death. The surviving individuals were continuously raised and their infection intensity was analyzed at 30 and 60 days, respectively. Severely infectious – indicates the number of individuals that were detected positive by 1st PCR. Slightly infectious – indicates the number of individuals that were detected positive by nested-PCR. Our analyses were performed with 3 shrimps from each tank and 5 replicates for each infection route (total 15 individuals).

Table 2. Gills from individuals that had died from YHV infection were collected at 12 and 24 hours post-mortem, and the homogenate was injected into the muscle of eight healthy individuals. The number of dead/surviving individuals and their infection intensity was recorded.

	12 hours later				24 hours later			
	Severely infected	Slightly infected	Undetectable	Total	Severely infected	Slightly infected	Undetectable	Total
Number of deaths	8	0	0	8	1	0	0	1
Survivors	0	0	0	0	0	2	5	7

Dead individuals were analyzed immediately after death. The surviving individuals were analyzed at 16 days.

D-01

Dissemination of a food commodity supply and demand model for ASEAN countries through an instruction manual

Future trends in food supply and demand have been gaining attention among ASEAN countries where agricultural trade liberalization is expected because of the establishment of the ASEAN Economic Community in 2015. In line with this, JIRCAS built an econometric model, i.e., a middle-term non-equilibrium supply and demand model, for making future projections related to agro-food products, and an instruction manual was subsequently published to facilitate dissemination. The know-how about the model had already been transferred to government officers in ASEAN countries through collaboration with the ASEAN Food Security Information System (AFSIS). The manual would be useful to officers, researchers, and students who are interested in understanding, building, and utilizing the model.

The manual contains the conceptual diagram (Fig. 1), the model structure expressed in an Excel worksheet (Fig. 2), and the projection results of the model (Fig. 3) as well as examples of scenario analyses. The non-equilibrium model in this manual does not presume equilibrium of food supply and demand in the domestic market, and would be the foundation for understanding more complicated models like the partial-equilibrium model often used by international organizations such as the Organization for Economic Cooperation and Development, Food and Agriculture Organization (OECD-FAO).

The manual shows how to use the model for policy evaluation and for comparative statics or welfare analysis. It also explained the basic concepts of econometrics required to develop the model including regression analysis, the adjusted coefficient of determination, and the standard error. In addition, for AFSIS project participants, the methods used to run the programs in developing and utilizing the model are further described.

The manual was published and disseminated to government staffs of ASEAN member states who participated in the project. It can also be downloaded from the AFSIS website (http://www.aptfsis.org/). It must be noted, however, that readers and users need to scrutinize the data and parameters in the manual, as these were collected and estimated by project participants. To produce better information from the analysis, provincial-level or more site-specific data should be used to build the model rather than the country-level model referenced in the manual. Furthermore, the model can be extended to partial-equilibrium models, where the effects of supply-demand balance on food prices are highlighted.

(E. Kusano, S. Shiratori, J. Furuya)

D-01

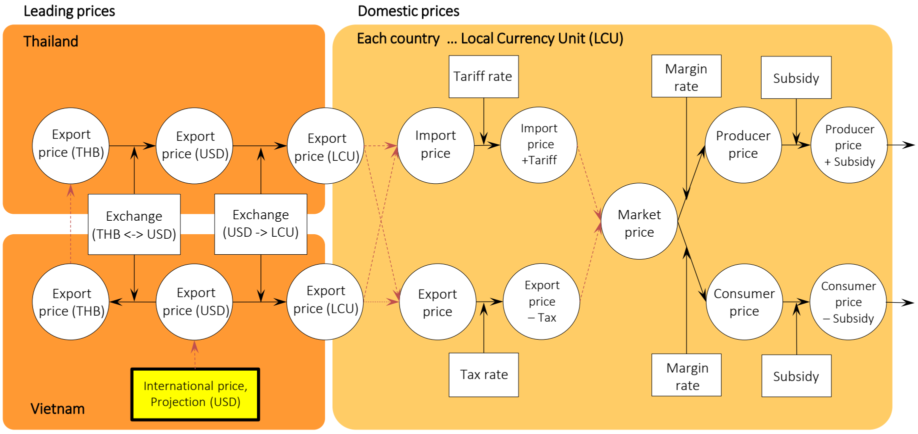

(a) Price linkage

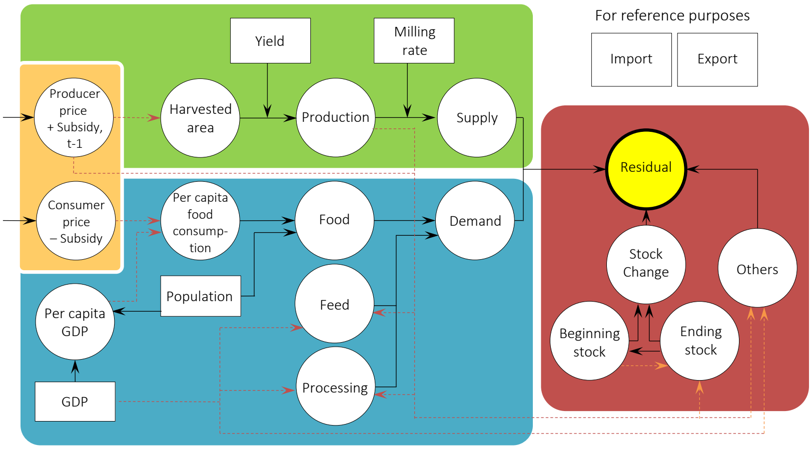

(b) Food balance sheet

Fig. 1. Conceptual diagram of the model (USD: US dollar, THB: Thai baht, LCU: Local currency unit)

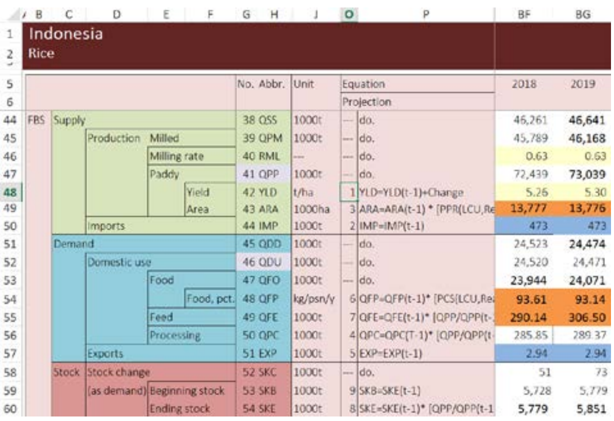

Indonesia
Rice

Row	Item			No.	Abbr.	Unit		Equation / Projection	2018	2019
44	FBS	Supply		38	QSS	1000t	—	do.	46,261	46,641
45		Production	Milled	39	QPM	1000t	—	do.	45,789	46,168
46			Milling rate	40	RML	—	—	do.	0.63	0.63
47			Paddy	41	QPP	1000t	—	do.	72,439	73,039
48			Yield	42	YLD	t/ha	1	YLD=YLD(t-1)+Change	5.26	5.30
49			Area	43	ARA	1000ha	3	ARA=ARA(t-1) * [PPR(LCU,Re	13,777	13,776
50		Imports		44	IMP	1000t	2	IMP=IMP(t-1)	473	473
51		Demand		45	QDD	1000t	—	do.	24,523	24,474
52		Domestic use		46	QDU	1000t	—	do.	24,520	24,471
53			Food	47	QFO	1000t	—	do.	23,944	24,071
54			Food, pct.	48	QFP	kg/psn/y	6	QFP=QFP(t-1)* [PCS(LCU,Re	93.61	93.14
55			Feed	49	QFE	1000t	7	QFE=QFE(t-1)* [QPP/QPP(t-	290.14	306.50
56			Processing	50	QPC	1000t	4	QPC=QPC(T-1)* [QPP/QPP(t-	285.85	289.37
57		Exports		51	EXP	1000t	5	EXP=EXP(t-1)	2.94	2.94
58		Stock	Stock change	52	SKC	1000t	—	do.	51	73
59		(as demand)	Beginning stock	53	SKB	1000t	9	SKB=SKE(t-1)	5,728	5,779
60			Ending stock	54	SKE	1000t	8	SKE=SKE(t-1)* [QPP/QPP(t-1	5,779	5,851

Fig. 2. Sample spreadsheet data and equations for the model

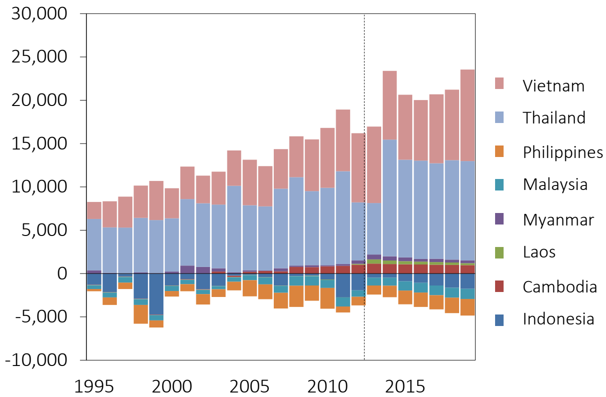

Fig. 3. Estimated surplus in rice supply (2012-2019) (1000t)

D-02

‘Sunny Shine’: A new passion fruit cultivar with low acidity and good appearance

In Japan, passion fruit (*Passiflora edulis*) ranks third in production among tropical fruits after pineapple and mango. It is produced mainly in the southern areas and consumed as fresh fruits, juice, and for processing. Some of the problems with fresh fruit consumption are immature fruit drop during periods of high temperature (above 30^{o}C) and high acidity after harvest. All conventional cultivars that were examined had the same problem.

To cope with these problems, JIRCAS developed the new passion fruit cultivar ‘Sunny Shine,’ which produces fruits that have lower acidity and good appearance. It was selected from seedlings obtained from a cross between JTPF-009 and ‘Summer Queen.’ JTPF-009 is a variety with a non-abscising fruit while ‘Summer Queen’ is a major passion fruit cultivar in Japan. The fruit quality and cultural performance were evaluated until 2015. In 2016, the new cultivar was named ‘Sunny Shine’ and an application for registration was filed (application number: 30972) in accordance with The Plant Variety Protection and Seed Act of Japan.

The average fruit weight of ‘Sunny Shine’ is about 110g (Table 1). The fruit color is red-purple with a smooth and glossy skin (Fig. 1). The matured fruit juice brix is about 18. The acidity of matured fruit juice during high temperature season is 1.5 to 2.0%, which is much lower than that of ‘Summer Queen’ (>2.0%), though there is no difference in juice acidity during low temperature season. ‘Sunny Shine’ has less immature fruit drop than ‘Summer Queen’ during high temperature season resulting in good coloring of the skin (Fig. 3). Days from flowering to fruit drop is longer in ‘Sunny Shine’ than ‘Summer Queen’ (Table 1) probably because it partly inherited the non-abscising characteristic of JTPF-009, resulting in lower acidity and less immature fruit drop. However, the cultural performance of ‘Sunny Shine’ is quite different depending on soil condition. The types of suitable soil and appropriate cultural management for growing ‘Sunny Shine’ are is under examination.

‘Sunny Shine’ is suitable for fresh fruit consumption because of its relatively large fruit size, good aroma, high brix, lower acidity during high temperature season, and glossy appearance. The development of this new cultivar with desirable traits will enhance production and consumption of passion fruit in Japan.

(T. Ogata, S. Yamanaka, H. Takagi, N. Kozai [National Agriculture and Food Research Organization], Y. Yonemoto [Yonetropics])

Table 1. Characteristics of ‘Sunny Shine’ and ‘Summer Queen’ (2013-2015)

Month	Cultivar	Days from flowering to harvest	Yield (kg/tree)	Fruit weight (g)	Pulp & seed (%)	Brix	Acidity (%)	Sugar-acid ratio
5	Sunny Shine	62	0.27	131	43.1	17.3	3.4	5.2
	Summer Queen	64	1.38	117	46.6	18.0	2.9	6.7
6	Sunny Shine	65	2.00	113	48.3a	18.2	2.2a	8.7a
	Summer Queen	62	2.62	110	46.8b	18.4	2.8b	6.8b
7	Sunny Shine	76a	2.04a	109a	55.1a	16.9a	1.5a	11.8a
	Summer Queen	55b	1.11b	98b	46.8b	17.9b	2.3b	8.1b
8	Sunny Shine	98	0.38	110	54.4	15.5	1.5	10.8
	Summer Queen	-	-	-	-	-	-	-

a,b: Different letters indicate statistically significant differences ($p<0.05$)

Fig. 1. Mature fruits of ‘Sunny Shine’ (top) and ‘Summer Queen’ (bottom)

Fig. 2. Fruit cross sections of ‘Sunny Shine’ (left) and ‘Summer Queen’ (right)

Fig. 3. Mature fruit color of ‘Sunny Shine’ (top) and ‘Summer Queen’ (bottom) during high temperature period